Jet-Cooled Electronic and Vibrational Spectroscopy of Crown Ethers: Benzo-15-Crown-5 Ether and 4′-Amino-Benzo-15-Crown-5 Ether

V. Alvin Shubert,[†] William H. James III, and Timothy S. Zwier*

Purdue University, Department of Chemistry, West Lafayette, Indiana 47907-2084

Received: May 6, 2009

Laser-induced fluorescence (LIF), ultraviolet hole-burning (UVHB), and resonant ion-dip infrared (RIDIR) spectroscopies were carried out on isolated benzo-15-crown-5 ether (B15C) and 4′-amino-benzo-15-crown-5 ether (ABC) cooled in a supersonic expansion. Three conformational isomers of B15C and four of ABC were observed and spectroscopically characterized. Full optimizations and harmonic frequency calculations were undertaken for the full set of almost 1700 conformational minima identified in a molecular mechanics force field search. When compared with TDDFT predictions, the S_0-S_1 origin positions serve as a useful diagnostic of the conformation of the crown ether near the phenyl ring responsible for the UV absorption and to the position of the NH_2 substituent. In-plane orientations for the β carbons produce red-shifted S_0-S_1 origins, while out-of-plane "buckling" produces substantial blue shifts of 600 cm^{-1} or more. Comparison between the alkyl CH stretch spectra of B15C and ABC divide the spectra into common subgroups shared by the two molecules. The high-frequency CH stretch transitions (above 2930 cm^{-1}) reflect the number of CH···O interactions, which in turn track in a general way the degree of buckling of the crown. On this basis, assignments of each of the observed conformational isomers to a class of structure can be made. All the observed structures have some degree of buckling to them, indicating that in the absence of a strong-binding partner, the crown folds in on itself to gain additional stabilization from weak dispersive and CH···O interactions.

I. Introduction

Since Pedersen's discovery in 1967,[1] crown ethers have become an important class of molecules noted for their ability to selectively bind guest substrates.[2,3] Important examples of this selectivity include the preferential binding of the Na^+ and K^+ cations to 15-crown-5 and 18-crown-6 ethers, respectively.[3] The cyclic structure of the crown ethers, with multiple oxygen sites facilitating the formation of well-defined "pockets", make them ideal molecules for studies of substrate binding. They also serve as useful models for enzyme binding[2] and can aid ion transport across membranes.[4,5] The selectivity of crown ethers in binding provides a chemical means for the extraction and sequestering of ions[6,7] and molecules,[8] leading to use in a diverse array of important applications including environmental cleanup as scavengers for 1.5 cesium and strontium,[6] potential uses in medicine,[9] and analytical and electronic uses as molecular photoswitches.[10] For the latter three purposes, the crowns must incorporate into their structure a chromophore, with benzene as a prototypical member, forming the benzo crown ethers that are the subject of the present study.

Given the important roles played by crown ethers, a vast literature exists describing their uses and properties. A full review of this literature lies outside the scope of this paper, but those relevant to the work presented here include a number of experimental[11−24] and theoretical[11,12,25−30] investigations of their fundamental properties. Much of this work has focused on crown complexation with ions[1,11,12,17,21,22,24,28] and neutral molecules,[13,15,16,18−21,26] while others attempted to gain insight into the preferred conformations of bare crown ethers.[14,18,23,25−27,29,30] Due to the experimental difficulties of probing the individual conformations of these molecules, most studies on uncomplexed crown ethers have been largely computational in nature. The computational studies on the 9-crown-3,[30] 15-crown-5,[29] and 18-crown-6 ethers[25,27] were focused on searching for low-energy minima.

Not surprisingly, these studies concluded that crown ethers are flexible molecules with potential energy landscapes characterized by a large number of low-lying minima. To make tractable an exhaustive search for conformational minima, all four of the studies mentioned above employed a molecular mechanics force field approach before application of any higher level methods.[25,27,29,30] These computational studies on isolated crown ethers generally found only a few very-low-energy minima (<∼4 kJ/mol), but several dozen below 12 kJ/mol.

Recently, Ebata and co-workers reported the jet-cooled conformation specific electronic and vibrational spectra of isolated crown ether molecules, involving benzo-18-crown-6 (B18C6) and dibenzo-18-crown-6 (DB18C6) and their water containing complexes.[18] The results for B18C6, which are most directly relevant to the present study, found four conformational isomers, one of which was assigned to a structure containing an all-planar arrangement for the dimethoxybenzene "core". The three other conformations with electronic origins shifted to higher frequency by almost 500 cm^{-1} were thereby characteristic of a less planar arrangement of this dimethoxybenzene moiety. More specific assignments were not attempted but nevertheless provide an important point of comparison with the present work.

The chemical structure of crown ethers such as 15-crown-5 (present in both benzo-15-crown-5 (B15C) and 4′-aminobenzo-15-crown-5 (ABC) ethers, see Scheme 1) might give the impression of a rigid, cyclic structure. However, as mentioned above, in the absence of a substrate, the crown ether is extremely flexible and we shall see shortly that the 15-crown-5 macrocycle

* To whom correspondence should be addressed. E-mail: zwier@purdue.edu.
[†] Current address: Argonne National Laboratory, Chemical Sciences and Engineering Division, Argonne, IL 60439.

10.1021/jp904231d CCC: $40.75 © 2009 American Chemical Society
Published on Web 06/24/2009

SCHEME 1

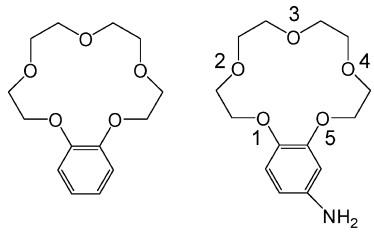

B15C ABC

has nearly 1700 stable conformational minima at the levels of theory employed herein. Substitution of the NH_2 group in the 4′ position on the aromatic ring produces 4 conformers of ABC for every asymmetric B15C structure and 2 for every symmetric B15C structure. The pyramidal character of the $C_\phi-NH_2$ group splits structures with the same crown cycle conformation into those with the NH_2 lone pair pointing up or down. In asymmetric B15C structures, two more unique ABC conformers are formed by reflecting the crown structure through a plane perpendicular to the plane of the phenyl ring, bisecting O(1) and O(5). This situation makes full characterization of the potential energy surfaces for B15C and ABC a time-consuming task with state-of-the-art computational methods. From an experimental standpoint, previous condensed phase crown ether studies have been unable to spectroscopically distinguish individual conformational isomers. Thus, there is still much to be learned about the inherent conformational preferences of bare crown ethers, their relative populations, interconversion barriers and rates, and spectroscopic signatures of the individual conformations.

Here, we present a detailed study of the infrared (IR) and ultraviolet (UV) spectra of individual conformational isomers of the two isolated 15-crown-5 ethers shown in Scheme 1, B15C and ABC. The phenyl ring incorporated into these crown ethers provides the ultraviolet chromophore necessary for the conformation-specific methods utilized in this work. These methods employ UV excitation and detection using either laser induced fluorescence (LIF) or resonant two-photon ionization (R2PI). Double resonance techniques are used to record the IR and UV spectra of the individual conformations.

As was observed in other molecules containing an oxygen linkage between chromophore and side chain,[31,32] the UV spectrum is sensitive to the conformation of the side chain to which the phenoxy moiety is attached. This sensitivity is used as a diagnostic for conformational assignment in this study. Furthermore, the alkyl CH stretch region of the infrared also holds clues to the macrocycle conformation via its CH···O interactions. When combined, the single-conformation spectra provide a general characterization of the preferred conformations of the uncomplexed 15-crown-5.

This study serves as a necessary foundation for single-conformation studies of the crown ethers bound to one or more binding partners. A fundamental question to be addressed in such studies is the extent to which the same conformations that dominate the bare crown ether appear in the crown-binding partner complexes, a task taken up in our study of the important case of crown−water complexes.[33]

II. Methods

A. Experimental Section. B15C (>99% purity) and ABC (97% purity) were used as supplied (Sigma Aldrich). The experimental apparatus used for LIF and R2PI studies have been previously described.[32,34] Aspects important to the present study are briefly reviewed here. The crown ether of interest was introduced into the vacuum chamber by passing a buffer gas over the heated (145 °C) sample reservoir and expanding the mixture through a pulsed valve with 0.8 mm orifice (Parker General Valve Series 9, 20 Hz) to create a supersonic expansion. For the LIF experiments, the He buffer gas was held at 2.3 bar with a typical flow of 0.6 (bar·cm^3)/s. For the R2PI experiments, the buffer gas (70% Ne/ 30% He) was held at 2 bar with a typical flow of 0.1 (bar·cm^3)/s.

The UV laser sources were the doubled outputs of Nd:YAG (Continuum 7000 series, Quantel Brilliant B) pumped tunable dye lasers (Lambda-Physik ScanmatePro, Scanmate, Lumonics Hyperdye). Ultraviolet spectra containing contributions from all conformations present in the expansion were recorded by employing LIF, while conformation-specific electronic spectra were obtained via UV−UV hole-burning (UVHB). In the latter method, a higher power hole-burning laser (10 Hz) was fixed on a transition observed in the LIF spectrum and a probe laser (20 Hz) was scanned over the wavelength region of interest. The hole-burning transitions used in the reported spectra, marked by asterisks on the appropriate figures, were the S_0-S_1 origins in all cases except ABC(*D*). The hole-burning and probe lasers were copropagated by use of a 50/50 beam splitter (CVI laser), spatially overlapped, and temporally separated such that the hole-burning laser preceded the probe by 200 ns. The hole-burning spectra were recorded by monitoring, via active baseline subtraction, the difference between the fluorescence signal from the probe laser with the hole-burn laser "on" or "off". All bands that originate from the same ground state level as the transition on which the hole-burning laser was fixed appeared as depletions in the fluorescence signal or ion signal.

Tunable infrared radiation from 2750−3600 cm^{-1} was produced with a seeded Nd:YAG pumped parametric converter (LaserVision, KTA based, 10 Hz) with typical IR laser powers of 1−5 mJ/pulse. The tuning range of the parametric converter was extended to produce mid infrared radiation over the range 1000−1600 cm^{-1} using a $AgGaSe_2$ crystal.[35] Typical laser powers achieved in this region were 100−150 μJ/pulse. Conformation-specific IR spectra were obtained via resonant ion dip infrared (RIDIR) and fluorescence dip infrared (FDIR) spectroscopies.[36,37] The IR and probe UV lasers were counter-propagated, spatially overlapped, and temporally separated so that the IR laser preceded the probe by 200 ns. The probe laser wavelengths were fixed on the same transitions in the electronic spectra as were used for UVHB. IR transitions arising from the same ground state level as the probe laser produced depletions in the probe signal. As in UVHB, active baseline subtraction was used to record the difference between IR laser "on" or "off".

B. Computational Methods. Given the anticipated complexity of the crown conformational potential energy surface, we adopted a strategy of using a classical force field to perform an initial search for conformational minima. The minima located using the force field were then used to initialize a hierarchical scheme for further geometry optimizations and vibrational frequency calculations with the Becke3LYP (B3LYP) density functional method[38,39] (DFT). Finally, single-point second-order Möller−Plesset perturbation theory[40] (MP2) energies were calculated.

The MMFs[41−45] force field was used as implemented in Macromodel 7.1[46] to perform the initial conformational search (10 000 iterations, 10 000 steps, 0.0001 convergence on gradient, 100 kJ/mol energy window) on B15C. All 2206 minima found with the force field were reoptimized at the B3LYP/6-31+G(d) level with *loose* optimization criteria and the *default* grid. A total of 1698 unique minima[47] (with 206 below 20.0 kJ/mol

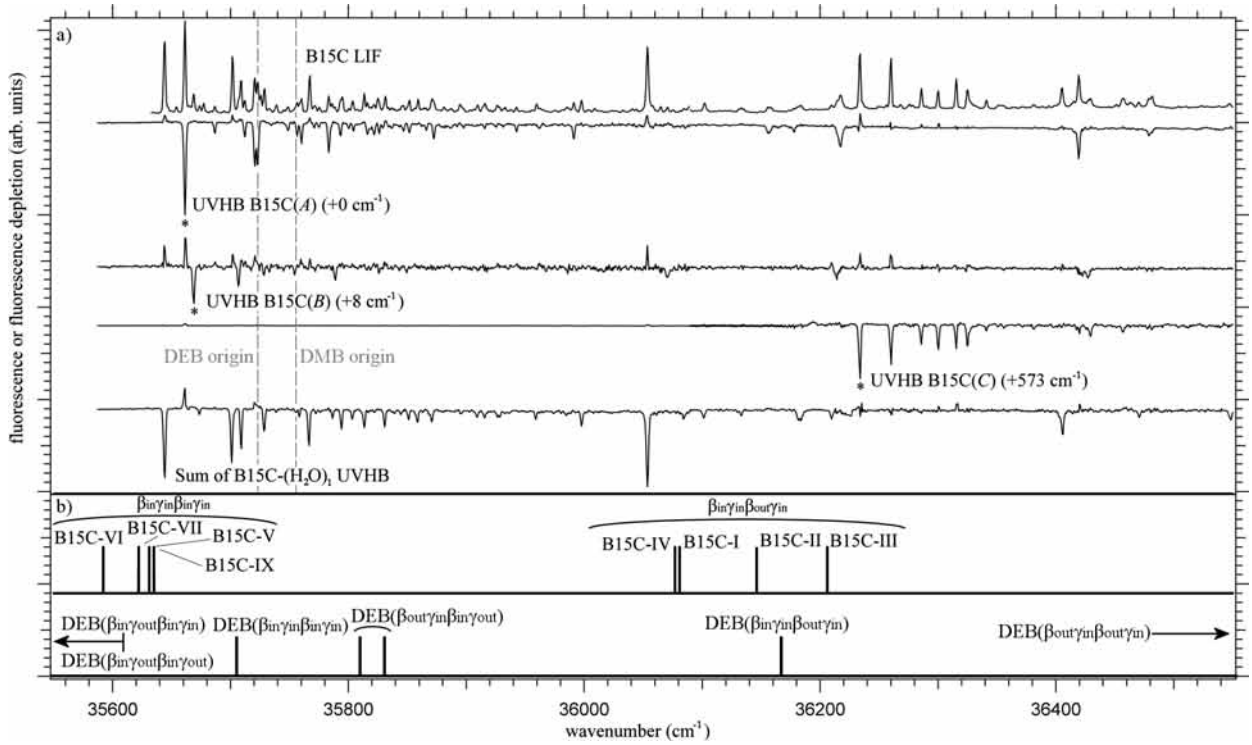

Figure 1. (a) LIF and UVHB of B15C in the S_0-S_1 region. Transitions used for UVHB are marked with asterisks. (b) Stick spectra of TDDFT predicted S_0-S_1 transitions for the low-energy conformations of B15C (upper trace) and prototypical DEB structures (lower trace).

before zero-point correction) were determined by comparison of relative energies (tolerance 0.01 kJ/mol) and rotational constants (sum of absolute values of percent differences between isoenergetic structures with a tolerance of 5%). A total of 207 unique low-lying structures were further optimized using B3LYP/6-31+G(d) DFT with an *ultrafine* grid and *tight* optimization criteria. A less exhaustive search was carried out on ABC, with 447 combined structures from a force field search and intuitive construction optimized at the default B3LYP/6-31+G(d) level. *Tight* optimizations with an *ultrafine* grid were carried out on the subset of these structures relevant to assignment.

Harmonic vibrational frequencies for the minima within 20 kJ/mol of the global minimum were calculated at the DFT B3LYP/6-31+G(d) level and single point MP2 energies at the B3LYP/6-31+G(d) geometry were calculated using the aug-cc-pVDZ basis set, both employing an *ultrafine* grid. All B3LYP and MP2 calculations were performed with the GAUSSIAN 03 suite of programs.[48] To predict the relative populations of the crown ether conformations prior to supersonic expansion, free energy corrections at the experimental source temperature were calculated using the unscaled B3LYP harmonic frequencies and rotational constants using a FORTRAN code developed for the purpose, which employed standard thermochemistry equations.[49]

Two further series of calculations were performed on the low-lying B15C reoptimized minima as an aid to making conformational assignments. Single point time-dependent DFT (TDDFT) calculations were carried out at the B3LYP/6-31+G(d) optimized structures (*ultrafine* grid, *scf=tight*). In a previous study on molecules with side chains bonded to a benzene chromophore through an oxygen linkage,[32] we found that TDDFT gave relative S_0-S_1 energy separations consistent with optimized resolution of the identity approximate couple clusters singles and doubles (RICC2) calculations,[50] and thus proved useful in arriving at a self-consistent set of conformational assignments.

To assess the source of the observed conformation specific shifts on S_0-S_1 energy separations, TDDFT calculations were also carried out on an analogous series of smaller molecules, methoxybenzene (MB), ethoxybenzene (EB), 2-phenoxyethanol (2PE), 2-(methoxyethoxy)benzene (2MEB), 1,2-dimethoxybenzene (DMB), 1,2-diethoxybenzene (DEB), 1,2-bis(2-hydroxyethoxy)benzene (BHEB), and 2,6-dimethylanisole (DMAS). Various prototypical conformations of each molecule were optimized (B3LYP/6-31+G(d) with the same optimization and grid criteria as above) locating local minima that could then be subjected to TDDFT single-point calculations at the optimized ground state geometry. These calculations provided a framework from which conformational assignments in B15C and ABC could be made and observed shifts in origins explained.

III. Results and Analysis

A. Ultraviolet and UV Hole-Burning Spectroscopy of B15C and ABC. Figures 1 and 2 present the LIF and UVHB spectra of B15C and ABC, respectively. The B15C UVHB spectra resolved transitions due to three monomer conformations. Mass selective resonant two photon ionization studies verified that the remaining transitions were due to B15C$-(H_2O)_1$ complexes that arose from residual water in the sample and gas lines (bottom trace). The S_0-S_1 origin transitions occur at 35 645, 35 653, and 36 217 cm^{-1} for the monomer conformers denoted A, B, and C, respectively. While the origins for B15C(A) and B15C(B) are separated by only 8 cm^{-1}, that for B15C(C) occurs over 550 cm^{-1} to the blue of A and B, a surprisingly large shift that should offer some clues to the conformational structure.

In fact, the S_0-S_1 origin positions of the conformations provide a sensitive probe of the structure substituents in the immediate vicinity of the phenyl ring responsible for the ultraviolet excitation, a fact recently exploited by Kusaka et al.

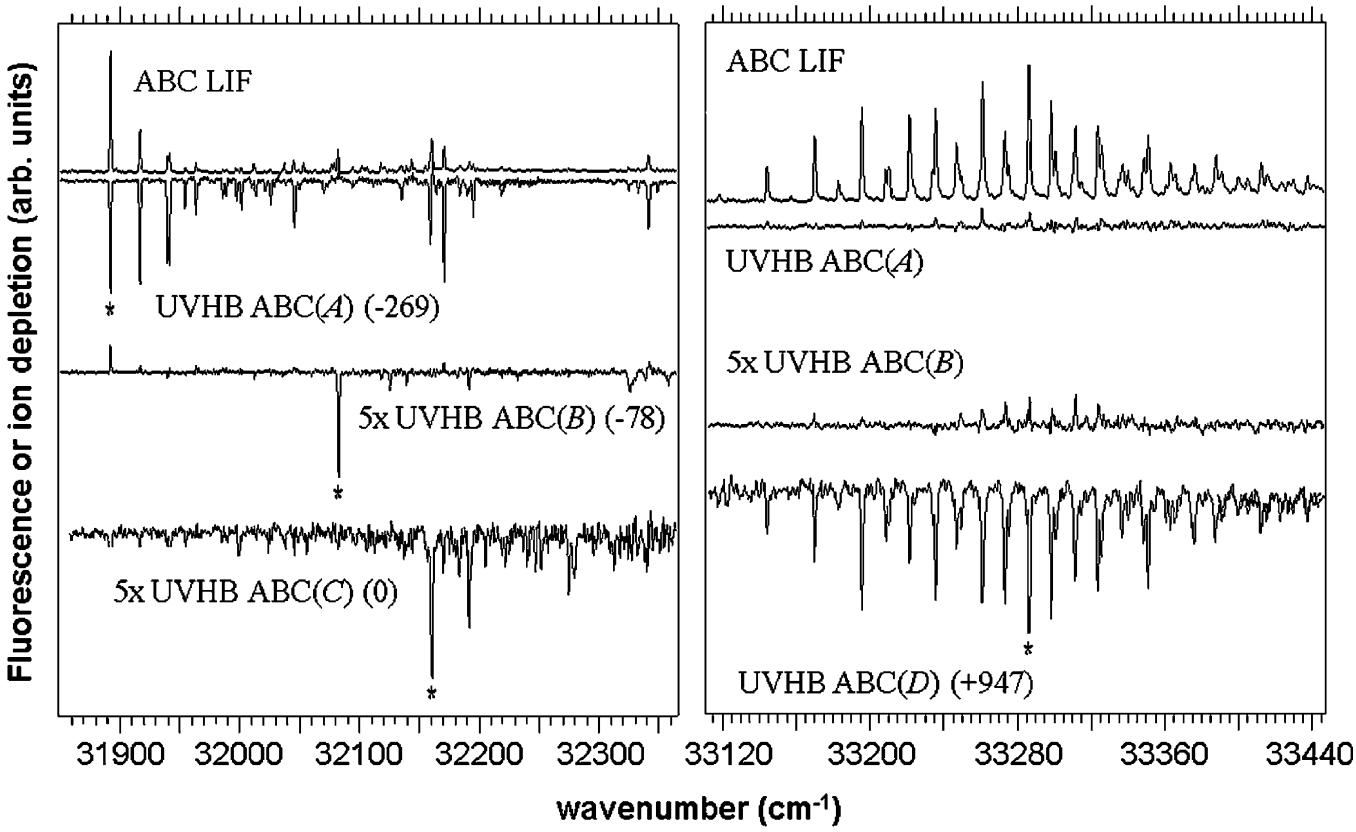

Figure 2. LIF and UVHB of ABC in the S_0-S_1 region. Transitions used for UVHB are marked with asterisks.

SCHEME 2

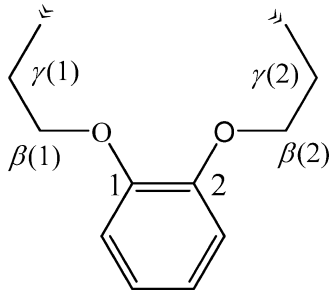

in their dibenzo-18-crown-6 ether (DB18C6)[51] and in our study of phenyl and phenol derivatives.[32]

In particular, TDDFT calculations predict that structures in which one of the β carbons (Scheme 2) is perpendicular to the plane of the phenyl ring will have S_0-S_1 origins shifted to the blue by several hundred cm^{-1} relative to their all in-plane counterparts. Kusaka et al. surmised from their TDDFT results that the observed conformations of DB18C6 had locally in-plane structures about one, and perhaps both, phenyl rings, although no direct experimental evidence for that correlation was presented.[51] In our study with phenoxy derivatives, we observed the same trend in the TDDFT results for out-of-plane β carbons as well as a red shift of several hundred cm^{-1} for out-of plane γ carbons.[32]

To extend these arguments to B15C, it is important to establish the positions of the S_0-S_1 origins of simpler analogs with known structures of the two alkoxy chains shown in Scheme 2. Figure 3 shows the R2PI spectra of 1,2-dimethoxybenzene (DMB) (Figure 3a) and 1,2-diethoxybenzene (DEB) (Figure 3b) recorded for that purpose.

The R2PI spectrum of DMB is similar to the LIF excitation scan presented by Yi et al.,[52] while no previous reports of the

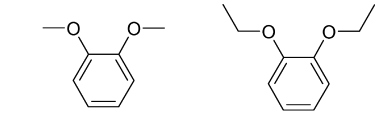

spectrum of DEB were found. The S_0-S_1 origin transitions of DMB and DEB are at 35 804 cm^{-1} and 35 712 cm^{-1}, respectively, values close to those for B15C(A) and B15C(B). On the basis of resolved rotational structure, Yi et al.[52] proved that DMB has both methyl groups in-plane, as shown in the inset to Figure 3a. The corresponding all in-plane structure for DEB (shown in the inset of Figure 3b) is the global minimum conformation. The close proximity of the S_0-S_1 origin of DEB to DMB makes it highly likely that the observed structure for DEB is this all in-plane structure. In fact, our scaled TDDFT calculations predict that the S_0-S_1 origin of this structure of DEB will be -57 cm^{-1} from DMB, close to its -39 cm^{-1} experimental difference.

The LIF and UVHB spectra of Figure 1 include dashed lines that mark the position of the S_0-S_1 origins of DMB and DEB. Their close proximity to the S_0-S_1 origin transitions of B15C(A) and B15C(B) (35 645 and 35 653 cm^{-1}, respectively) argues for all in-plane structures for these two conformers of B15C in the vicinity of the phenyl ring. Furthermore, the low-frequency vibronic features associated with torsions of the substituent chains for both B15C(A) and B15C(B) are similar to those observed in DEB (Figure 1 compared to Figure 3b), providing confirmatory evidence for our assignment.

To refine our structural deductions for B15C(A,B) and to establish the local structure responsible for the blue-shifted spectrum of B15C(C) (+572 cm^{-1} from B15C(A)), we carried out a systematic TDDFT study of the predicted S_0-S_1 origins of a series of eight close analogs of B15C, including various

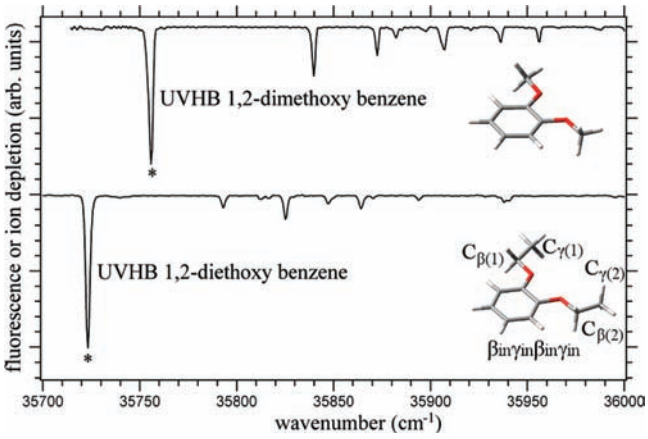

Figure 3. UVHB spectra and assigned structures of (a) 1,2-dimethoxybenzene (DMB) and (b) 1,2-diethoxybenzene (DEB).

in-plane and out-of-plane conformations of the C_β, C_γ, and next nearest neighbor oxygen atoms (Scheme 2). The results of this study are included in the Supporting Information.[53] Several trends in the dependence of the S_0-S_1 separation with substituent geometry emerged that strengthened and refined the qualitative interpretation of Kusaka et al.[51]

The predicted frequency shifts associated with various geometries of the two alkoxy chains of DEB are summarized in Figure 1b). In the figure, we use a short-hand notation in which the in-plane or out-of-plane positions of both C_β and C_γ are indicated. Relative to all-planar geometries, out-of-plane C_β's induce large blue shifts, while out-of-plane C_γ's that retain an in-plane C_β (i.e., $\beta_{in}\gamma_{out}$) induce smaller but still significant red shifts of the S_0-S_1 energy separations. In the doubly substituted molecules, the effects tend to be additive; e.g., structures with both C_β's out-of-plane produce a blue shift approximately double that induced by a single out-of-plane C_β. The same is true for the red shifts induced by out-of-plane C_γ's. Furthermore, if C_β of one chain is out-of-plane and the C_γ of the opposite chain is also out-of-plane, the net result is a small blue shift (<100 cm^{-1}) from the all-planar geometry. Overall, the anticipated shifts between different structural classes are large enough (on the order of hundreds to a thousand cm^{-1}) that inspection of the experimental origins relative to those recorded for DMB and DEB provides a means for categorizing the observed conformations into classes of structures and thereby reducing the number of candidate structures that need to be considered.

The TDDFT results suggest that the small red shifts of the S_0-S_1 origins of B15C(A,B) relative to DEB arise from structures in which one or both of the next oxygens are out-of-plane. A structure with only one of these oxygens out-of-plane would make it impossible to complete the crown cycle, and so both of the ring ethyl ether groups are assigned assuming an in/in/out geometry for the $C_\beta/C_\gamma/O$ atoms (see Table 1).

The experimental origin of B15C(C) occurs 498 cm^{-1} blue of DEB. The low-frequency vibronic activity near the B15C(C) origin is more extensive and intense than that observed for DEB, suggesting a significant difference from the all heavy atom planar arrangement of DEB. The direction of the origin shift indicates out-of-plane C_β's, while its magnitude is consistent with only a single C_β out-of-plane with an all-planar arrangement in the opposing $C_\beta-C_\gamma$ moiety. The out-of-plane C_β arrangement is also consistent with the increased amount of observed vibronic activity observed in the hole-burning spectrum of B15C(C) (Figure 1) due to the increased amount of interaction between the crown cycle and benzene π cloud. B15C(C) is thus assigned to a structure with an out/in; in/in arrangement.

The UVHB spectra for ABC (Figure 2) lend strong support to the above crown assignments near the phenyl ring. Four conformations of ABC were resolved with very large separations between the origin transitions. The origins of ABC(A) (31 879 cm^{-1}) and ABC(B) (32 068 cm^{-1}) are red-shifted by 278 and 89 cm^{-1} from ABC(C) (32 157 cm^{-1}), respectively, while ABC(D) (33 104 cm^{-1}) is blue-shifted by 947 cm^{-1}. ABC(B) and ABC(C) display vibronic activity similar to that observed in B15C(A) and B15C(B) while the UVHB spectrum of ABC(A) has vibronic activity similar to that for B15C(C). The hole-burning spectrum of ABC(D), with long, harmonic Franck−Condon progressions, indicates a large geometry change between the ground and excited states.

The substitution of the amino group on the phenyl ring produces shifts quite different than those in B15C, which are interpretable on the basis of previous studies of amino-substituted phenols and anisoles.[54−56] This comparison is made in detail in the Supporting Information.[53] For our purposes here, we surmise the following: the presence of the alkoxy group in the meta position relative to the amino group has a much smaller impact on shifting the S_0-S_1 origins than substitution in the para position. To a first approximation, in 3,4-dialkoxyanilines an origin near the *m*-aminophenol origin is expected if the C_β is out-of-plane on the para chain while an all-planar geometry of the chain para should give an origin near that of *p*-aminophenol.

The fact that the electronic origins of ABC(A), -(B) and -(C) occur nearly 1000 cm^{-1} to the red of ABC(D) is reminiscent of the shifts observed between *p*-aminophenol and *cis-m*-aminophenol.[54−56] These shifts strongly suggest that in ABC(A,B,C), the C_β of the crown cycle chain para to the amino group is nominally planar, while in ABC(D) this C_β is out-of-plane. This assignment is consistent with the vibronic activity of the electronic spectra. In fact, the similarities between the electronic spectra, apart from the positions of the origins, indicates the following tentative pairing between B15C and ABC conformers sharing the same crown conformation: ABC(B) with B15C(B), ABC(C) with B15C(A), and ABC(A) with B15C(C), respectively. For ABC(A), this would mean that the single out-of-plane C_β would be at the meta position relative to the amino group. Table 1 summarizes key computational and experimental data for the relevant conformations of B15C and ABC.

B. IR Spectra of B15C and ABC. Figure 4 compares the fluorescence-dip (B15C) or resonant ion-dip (ABC) IR spectra in the alkyl CH stretch region of B15C and ABC. Apparent from the spectra are near exact correspondences between the previously identified pairs of conformations of B15C and ABC. Since the alkyl CH stretch region is sensitive to the entire crown cycle conformation, the conformation-specific IR spectra unambiguously identify the presence of three unique crown conformations, one shared by B15C(A) and ABC(C), a second by B15C(B) and ABC(B), and a third taken up by B15C(C), ABC(A), and ABC(D). Thus, ABC(A) and ABC(D) share the same crown conformation, differing in whether the amino group is meta or para to the out-of-plane C_β while the opposite chain remains nominally planar near the phenyl ring.

The association of ABC(A,D) with B15C(C) confirms the initial assignment of B15C(C) to a structure with a single C_β out-of-plane. Furthermore, the large red shift of B15C(A,B) from B15C(C) together with their small observed vibronic activity strongly supports the assertion that both sides of the crown cycle in B15C(A,B) are planar near the phenyl ring. Finally, the IR spectra of B15C(A,B) and ABC(B,C) share many common features, particularly in the 2830−2930 cm^{-1} region, lending

TABLE 1: Summary of Experimental and Computational Data for ABC and B15C

structure (assignment), designation (B15C)[a] or B15C equivalent (ABC)[b]				η[c]	no. of CH > 2930 cm^{-1} (no. of CH•••O < 2.9 Å)	exp origin (cm^{-1})			TDDFT (cm^{-1})			ΔE (kJ/mol)		ΔG (kJ/mol)[h]
						absolute	relative to *A*	relative to DEB	scaled[d]	relative to *A*	relative to DEB/DEA[e]	B3LYP[f]	MP2[g]	
B15C	I (C)	**[g+g-a]**[ag-a][g-g+a] [g+g-a][g-g+a]		0.45	7 (4)	36217	572	505	36081	450	312	0.0	0.0	0.0
	II	**[ag+g-]**[aaa][g-g+a] [ag-a][ag+a]		0.91	2 (2)				36146	515	377	0.1	5.9	1.1
	III	**[ag-g+]**[ag+g-][ag-g+] [g-g-g+][g+g-a]		0.33	5 (5)				36206	575	437	9.9	5.0	4.6
	IV	**[g-g+a]**[ag-a][ag+g-] [ag-g-][g+g-a]		0.53	3 (3)				36077	445	308	6.5	7.4	4.7
	V (A)	**[ag+a]**[ag+a][g+aa] [g-g+a][ag-a]		0.91	3 (1)	35645	0	–67	35631	0	–138	1.5	8.2	4.4
	VI	**[ag+a]**[ag-g+][aaa] [g+g-a][ag+a]		0.90	2 (2)				35592	–39	–177	2.1	8.7	3.7
	VII (B)	**[ag-a]**[ag+g-][aaa] [ag+g-][ag-a]		0.82	2 (2)	35653	8	–59	35622	–9	–147	7.1	12.2	5.6
	VIII	**[ag-a]**[ag+a][ag-g+] [aag+][ag+a]		0.83	3 (1)				35465	–167	–304	9.9	13.4	9.8
	IX	**[ag-a]**[ag+a][g+g-g+] [g+ag+][g-g+a]		0.66	2 (2)				35635	4	–134	14.2	14.1	9.8
	X	**[ag-a]**[ag-a][ag+a] [ag-a][ag+a]		1.00	0 (0)				35432	–199	–337	3.7	15.0	11.7
ABC	I	(D)	(I)-y up	0.46	6	33104	1225		33040	1543	746	0.0	0.0	0.0
	II		(I)-y dn	0.46	6				33043	1545	749	0.0	0.0	0.0
	III	(A)	(I)-x up	0.45	6	31879	0		31497	0	–796	4.1	2.1	2.0
	IV		(I)-x dn	0.45	6				31293	–204	–1000	4.4	2.4	2.3
	V	(C)	(V)-x dn	0.91	3	32157	278		31625	128	–668	5.1	10.8	6.6
	VI		(V)-x up	0.91	3				31668	170	–626	5.4	11.1	6.8
	VII		(V)-y dn	0.91	3				31537	39	–757	5.6	11.2	7.0
	VIII		(V)-y up	0.91	3				31590	92	–704	5.8	11.4	7.2
	IX		(VII)-x dn	0.82	2				31487	–10	–806	11.1	14.8	7.5
	X		(VII)-x up	0.83	2				31529	32	–764	11.3	15.5	8.3
	XI		(VII)-y dn	0.82	2				31649	152	–644	10.6	14.9	8.2
	XII	(B)	(VII)-y up	0.83	2	32068	190		31654	157	–640	11.0	15.0	8.3

[a] Bold letters indicate conformation of the dimethoxyethane unit that included both aromatic carbons. See Supporting Information[53] for naming scheme explanation. [b] See Figure 6 for constructing ABC geometries from B15C by placing amino group at x or y positions. [c] "Buckling" parameter, described in eq 1. [d] See Supporting Information for TDDFT scaling information. [e] Scaled TDDFT relative to the results for the all heavy atom planar geometries of DEB or dimethoxyaniline (DEA). [f] Geometry optimized B3LYP/6-31+G(d) energies zero-point corrected with unscaled B3LYP/6-31+G(d) frequencies. [g] Single-point MP2/aug-cc-pVDZ energies zero-point corrected with unscaled B3LYP frequencies. [h] Free energy calculated with correction from unscaled B3LYP frequencies at the sample temperature (420 K) added to the single point MP2 energies.

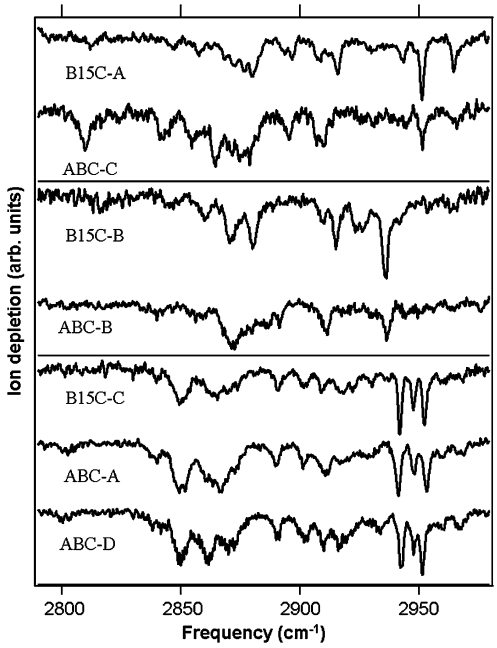

Figure 4. Comparison of the IR-dip spectra for B15C and ABC in the alkyl CH stretch region.

support to the assignment of these structures as having the same conformation on each side of the crown cycle out to the first nonaromatic oxygen as presumably many of the CH stretch transitions shared in common arise from these four methylene groups.

The alkyl CH stretch spectra contain contributions from all 16 alkyl CH stretch fundamentals that comprise the macrocycle. As a result, the spectra are sensitive to the entire crown cycle conformation regardless of proximity to the phenyl ring. These spectra are congested with broad features below 2930 cm^{-1} that arise from close-lying CH stretch fundamentals and overtones of CH bending modes that gain oscillator strength via Fermi resonance with the CH stretch modes. Generally speaking, the antisymmetric CH stretch modes of the CH_2 groups appear at higher frequency than the symmetric stretch modes, but these two regions overlap significantly and, with so many alkyl CH oscillators contributing to the spectrum, classification into symmetric and antisymmetric modes is often not possible. Furthermore, inspection of the calculated CH stretch normal modes indicates that the CH stretch motions of individual CH_2 groups are often partially localized on a single CH bond, while other normal modes distribute significant amplitude between several CH_2 groups in the crown. Anharmonic mixing of CH stretch and CH bend overtones adds further complexity to making quantitative comparison between experiment and calculation in the alkyl CH stretch region. As a result, a quantitative match between harmonic vibrational frequency calculations and experiment and theory is not expected. Consequently, we pursue a more qualitative measure of the crown conformation.

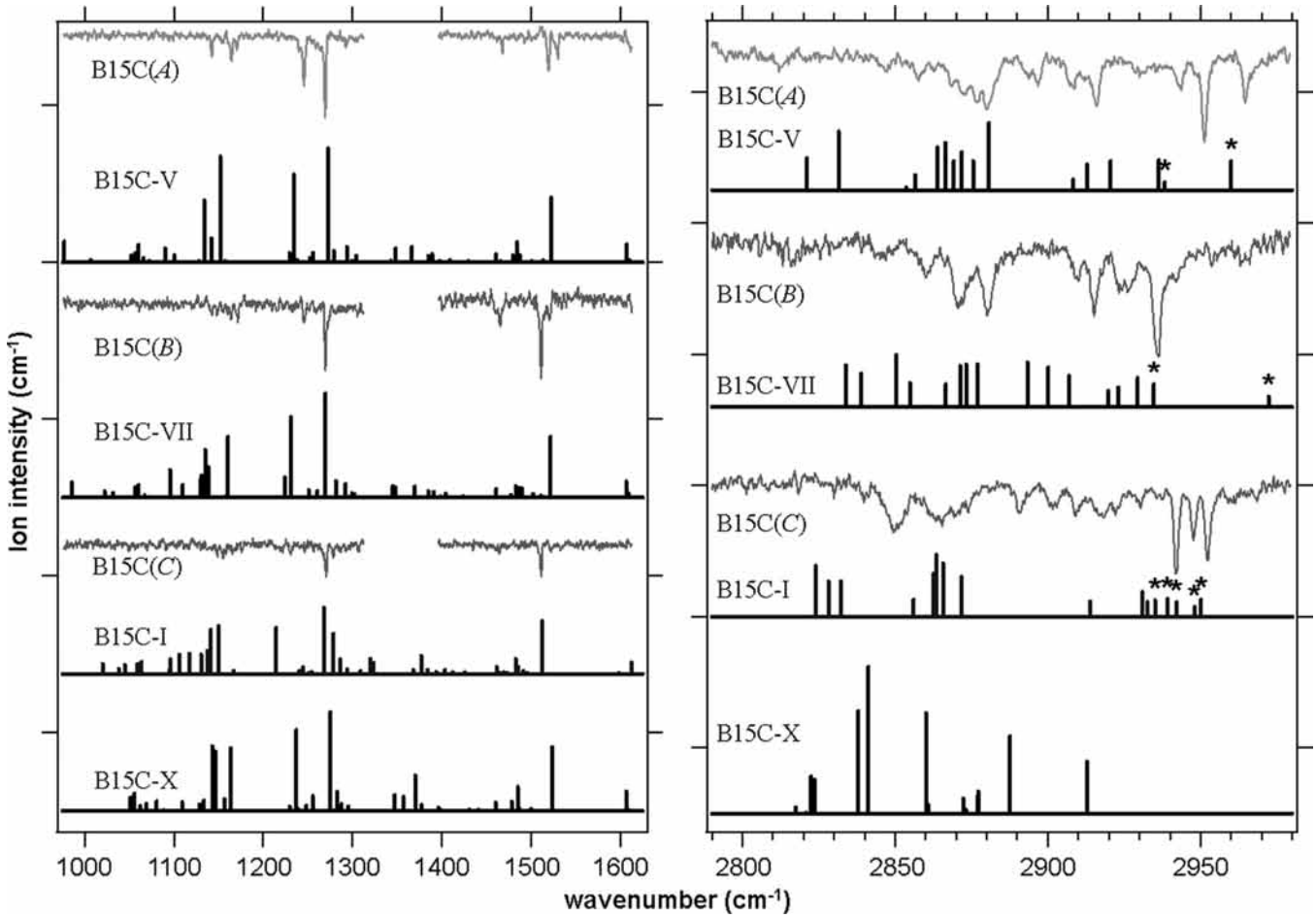

Figure 5. Comparison of experimental and calculated B15C RIDIR spectra. The left trace presents the CO stretch region with the calculated spectra scaled by 0.98. The right trace presents the CH stretch region with calculate spectra scaled by 0.95. Transitions arising from CH's involved in CH···O H-bonds are marked by asterisks.

The most striking differences between the three conformation-specific alkyl CH stretch spectra in Figure 4 occur in the less congested region above 2930 cm^{-1}, where one or more sharp transitions appear at unique wavenumber positions. In what follows, we seek to understand the source of these high-frequency CH stretch transitions and what they tell us about the conformations of the crown ethers.

Several previous studies of the infrared spectroscopy of CH groups in a variety of contexts have noted that CH stretch fundamentals shift to higher frequency when the CH group is involved in an interaction with an electronegative atom.[57−59] The presence of multiple oxygen sites in the crown cycles provides ample opportunity for the methylene hydrogens to take part in stabilizing CH···O interactions, although to do so requires the crown cycle to buckle in on itself. Figure 5 presents the calculated stick spectra for several low-energy B15C conformers. While B15C-I, -V, and -VII, with structures shown in Figure 6a−c, are partially buckled structures, B15C-X is a symmetric, open structure (Figure 7a) that does not allow for any significant CH···O interactions to occur. In the structures shown in Figures 6 and 7, CH groups in closest proximity to ether oxygens are linked to them by dotted lines, with the indicated H···O distances given below the structures. Atoms in molecules (AIM) calculations indicate that the total charge density at the intramolecular hydrogen bond critical point between the linked CH and O groups is characteristic of formation of a weak H-bond.[60] In keeping with this, the calculated infrared spectrum of the "open" crown structure in

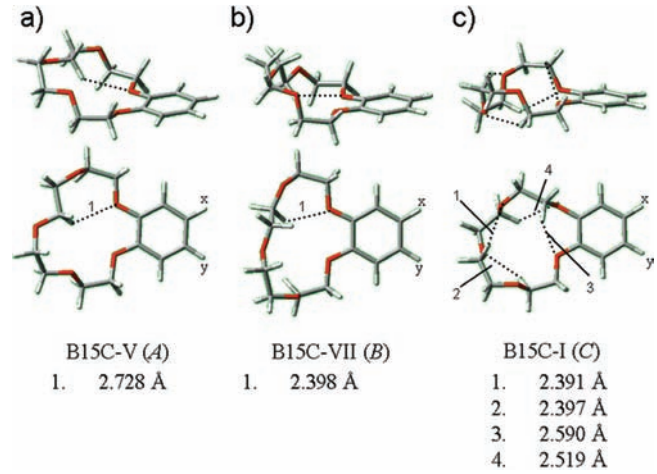

Figure 6. B15C structures consistent with the spectral data for the observed conformations. Positions for amino group substitution to form ABC structures are marked x and y. Amino lone pair "up" corresponds to a lone pair oriented toward the top of page for the side views or out of the page for the overhead views. See Table 1.

B15C-X (Figure 7a) shows no CH stretch activity above 2930 cm^{-1}, while the transitions on the high-frequency edge of the spectra marked by asterisks in conformers I, V, and VII are due to the CH groups involved in CH···O interactions. Thus, the calculated spectra are consistent with an interpretation of the presence of these sharp, high-frequency transitions as indicative of CH···O interactions, with the number of transitions

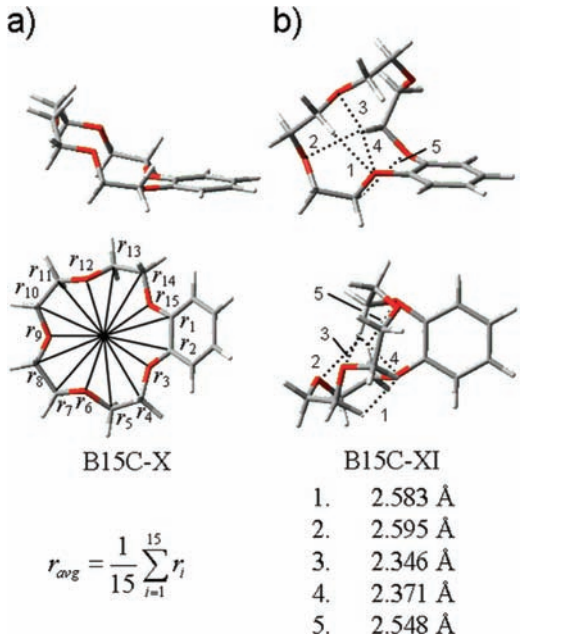

Figure 7. (a) Most open and (b) most "buckled" B15C structures found. In (a), solid lines denote distance from heavy atom to center of crown cycle structure. In (b), CH···O interactions are marked with dashed lines and corresponding H···O distances given.

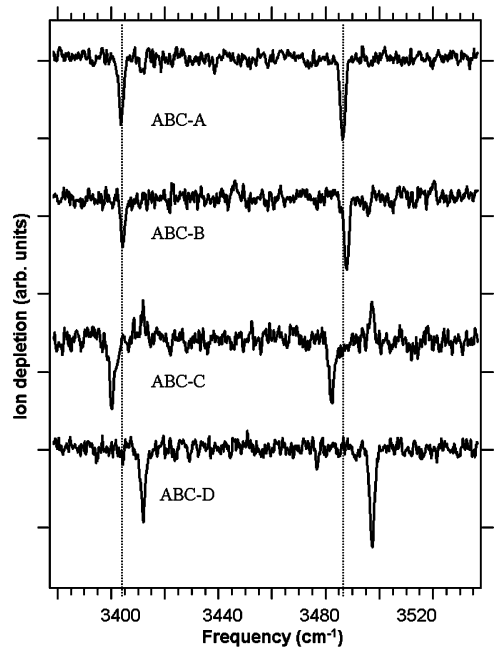

Figure 8. RIDIR spectra in the NH stretch region for ABC along with scaled (0.9616) calculated NH stretch stick spectra.

corresponding, at least qualitatively, to the number of such interactions and the amount of buckling of the crown cycle.

This interpretation is consistent with the partial structural assignments derived from the UVHB spectra. B15C(C) and ABC(A,D) contain three sharp transitions on the high-frequency side of the alkyl CH stretch region (Figure 4c), more than the number observed for the other two crown conformations (Figure 4a,b). A structure with an out-of-plane C_β should give rise to a more buckled crown structure that brings more of the oxygen atoms into close proximity with CH groups elsewhere in the cycle. In comparison, the nominally planar structures assigned to B15C(A,B) and ABC(B,C) would tend to keep the crown structure more open and provide fewer opportunities for CH···O interactions to occur. As a result, in arriving at structures I, V, and VII as structures consistent with experiment, we sought out structures with the appropriate near phenyl ring substructure assigned from the electronic spectra that contained the appropriate number of CH···O interactions.

B15C(A) and B15C(B) were both assigned to all-planar structures near the phenyl ring on both sides of the crown, with the first out-of-plane atom the first nonaromatic oxygens along each chain. Twenty such structures meeting these criteria were found within the 207 structures on which higher level calculations were performed. These structures generally have only 1 or 2 significant CH···O interactions (see, for example, Figure 6a,b), consistent with the expectations based on the IR spectra. While the computed harmonic spectra do not provide a one-to-one match-up with the observed spectra, they do show similar patterns with experiment, particularly in comparing B15C−V with B15C(A).

The case for assigning B15C(C) to B15C-I and ABC(A,D) to its 4′-amino counterparts is somewhat stronger, since B15C-I is the global minimum crown cycle structure at both the B3LYP and MP2 levels of theory and contains the appropriate structural criteria deduced from the electronic and IR spectra. As expected, this structure contains multiple CH···O interactions, and the CH stretches involved in CH···O interactions all appear in the high-frequency edge of the spectrum, marked by asterisks in Figure 5.

Figure 5 also presents the RIDIR spectra taken in the 1000−1600 cm^{-1} region where strong transitions due to CO stretching modes were predicted by the calculations. The most intense modes above 1200 cm^{-1} contain CO stretch and CH bend character, both involving an aromatic carbon. Several strong features appear in the spectra for each conformation in this region and although the differences between each spectrum are too small to definitively confirm the assignments, the assignments are consistent with the predicted spectra.

The amino group of ABC provides additional spectroscopic data not available in B15C. In asymmetric crown structures, four orientations of the amino group are possible, the two meta sites multiplied by two orientations of the nitrogen lone pair (either "up" or "down"). The nearly exact correspondence between the calculated alkyl CH stretch spectra for like crown cycle conformations of B15C and ABC demonstrates that the alkyl CH stretch spectra are insensitive to the amino group position and orientation. Thus, discrimination as to which of the positions and orientations to assign the ABC structures come from comparison of the electronic and RIDIR NH stretch spectra with the B3LYP DFT and frequency calculations as well the MP2 relative free energies.

Figure 8 presents the RIDIR spectra of ABC in the NH stretch region. The most striking difference between these spectra is the approximate 10 cm^{-1} shift to higher frequency of both of the symmetric and asymmetric stretches of ABC(D) from ABC(A,B,C). This shift confirms that the difference between the conformations ABC(A) and ABC(D) is associated with the amino group. The B3LYP DFT vibrational frequencies serve to confirm the assignments just made since, although the magnitude of the calculated shift is smaller than observed, DFT B3LYP/6-31+G(d) calculations do predict a blue shift of both NH_2 stretching modes in ABC-I and ABC-II relative to ABC-III and ABC-IV. Furthermore, NH stretches of *p*-aminophenol are red-shifted from *m*-aminophenol,[56] consistent with assignment of ABC(A) to the structure with an in-plane C_β bonded

TABLE 2: Summary of Experimental and Computational NH Stretch Data for ABC

		sym(NH_2)		asym(NH_2)	
structure	assignment	experimental	calculated	experimental	calculated
DEA			3399.7		3490.2
ABC-I	D	3412	3409.8	3497.3	3501.7
ABC-II			3410.1		3501.9
ABC-III	A	3403.6	3403.5	3486.3	3494.4
ABC-IV			3404.4		3495.4
ABC-V	C	3400.2	3401.8	3482.5	3492.4
ABC-VI			3403.3		3494.1
ABC-VII			3400.9		3491.4
ABC-VIII			3401.5		3492.0
ABC-IX			3401.4		3491.8
ABC-X			3401.5		3492.1
ABC-XI			3401.7		3492.2
ABC-XII	B	3404.4	3403.5	3487.9	3494.4

to the oxygen para to the NH_2 group and ABC(D) to the same crown conformation with the NH_2 group meta to this in-plane C_β. The predicted vibrational frequency shifts between the different ABC(B,C) candidate structures (ABC-V−XII) are small, on the order of 1−2 cm^{-1} and so do not allow with confidence any further refinement of the conformational assignments of ABC(B,C), although Table 2 associates the best matches together.

IV. Discussion and Conclusions

Single-conformation IR and UV spectroscopies were used to determine that jet-cooled benzo-15-crown-5 (B15C) and 4′-amino-benzo-15-crown-5 (ABC) are cooled into three and four conformational isomers, respectively. In some ways, this result is already noteworthy because DFT B3LYP/6-31+G(d) calculations predict the presence of almost 1700 distinct conformational isomers of B15C, over 200 of which have energies within 20 kJ/mol and 28 of these within 10 kJ/mol of the global minimum. This structural diversity is one of the hallmarks of the crown ethers, contributing to their ability to reshape themselves to accommodate binding partners of different sizes and interaction types (e.g., ionic or H-bonding). As a result, the barriers separating the minima are anticipated to be modest in size. Under such conditions, the collisional cooling that occurs in the supersonic expansion should funnel population initially present in higher-lying minima over the tops of these barriers to the lower-lying minima as cooling proceeds. However, the driving force is not large when the energy separation is small, and so it is still somewhat surprising that the resulting downstream populations in the expansion reside in only three (B15C) or four (ABC) minima.

At the same time, the alkyl CH stretch spectra of B15C and ABC have provided unequivocal evidence that the same crown ether structures are observed in both molecules, indicating a certain robustness to the observed conformational preferences and the cooling process that leads to the final conformer populations. What the present results do not provide is any direct experimental evidence for the relative energies of these minima, nor for the magnitudes of the barriers separating them. However, population transfer methods developed by our group[61−65] are capable of these measurements, and the conformation-specific spectroscopy described here provides the necessary foundation for such future work.

From a computational viewpoint, a strength of the calculations described in this work is their comprehensive nature, with converged structures for all 1698 minima[47] calculated at the DFT B3LYP/6-31+G(d) level of theory.[38,39] Higher level theory, which better describes dispersive interactions and minimizes intramolecular basis set superposition error (BSSE) are clearly warranted, as are calculations of the transition states separating them. Ultimately, a quantitatively accurate disconnectivity diagram for benzo-15-crown-5 would be a valuable addition on which simulations of conformational isomerization could be carried out.[66]

Given the extraordinary complexity of the potential energy surface of B15C and ABC and the limited nature of the spectroscopic handles available, we have taken an approach, similar to that of Ebata and co-workers,[18,51] in pursuing initial assignments to particular conformational families distinguished by the crown structure near the aromatic ring. Although we were able to extend these assignments to assess the general degree of buckling of the crown structure, we have not made unequivocal assignments for each observed conformer-specific spectrum to a single conformational isomer. To that end, we have used two highly complementary conformation-specific spectroscopic probes: the ultraviolet and the alkyl CH stretch infrared spectra.

The UVHB spectra identified the wavenumber positions of the S_0-S_1 origins for each conformer as well as the amount and type of torsional vibronic structure built off of these origins. Both aspects reflect the local conformation of the crown near the phenyl ring responsible for the electronic excitation. The positions of the S_0-S_1 origins are extraordinarily sensitive to the orientation of C_β and C_γ relative to the plane of the aromatic ring. Furthermore, in ABC, the S_0-S_1 origin was also sensitive to whether the first out-of-plane carbon in the crown was meta or para to the NH_2 group on the ring. Single-point TDDFT calculations faithfully reproduced these shifts for a large number of cases where experimental data was available, and consistently tracked the crown conformations shared by B15C and ABC. As a result, the S_0-S_1 origin positions served as a powerful diagnostic of the local conformation of the crown in the vicinity of the phenyl ring. On this basis, we deduced that B15C(A)/ABC(C) and B15C(B)/ABC(B) have all four of the closest alkyl carbons to the aromatic ring (the $\beta(1)$, $\beta(2)$, $\gamma(1)$, and $\gamma(2)$ carbons) in-plane with that ring, while B15C(C)/ABC(A,D) have one of the C_β in-plane and one out-of-plane, producing large shifts in the S_0-S_1 origin positions.

In contrast, the single-conformation IR spectra in the alkyl CH stretch region reflect the conformation of the entire crown structure, with contributions in principle from all 16 alkyl CH bonds in the crown. The spectra shown in Figure 4 reflect this high-information content, with spectral signatures of

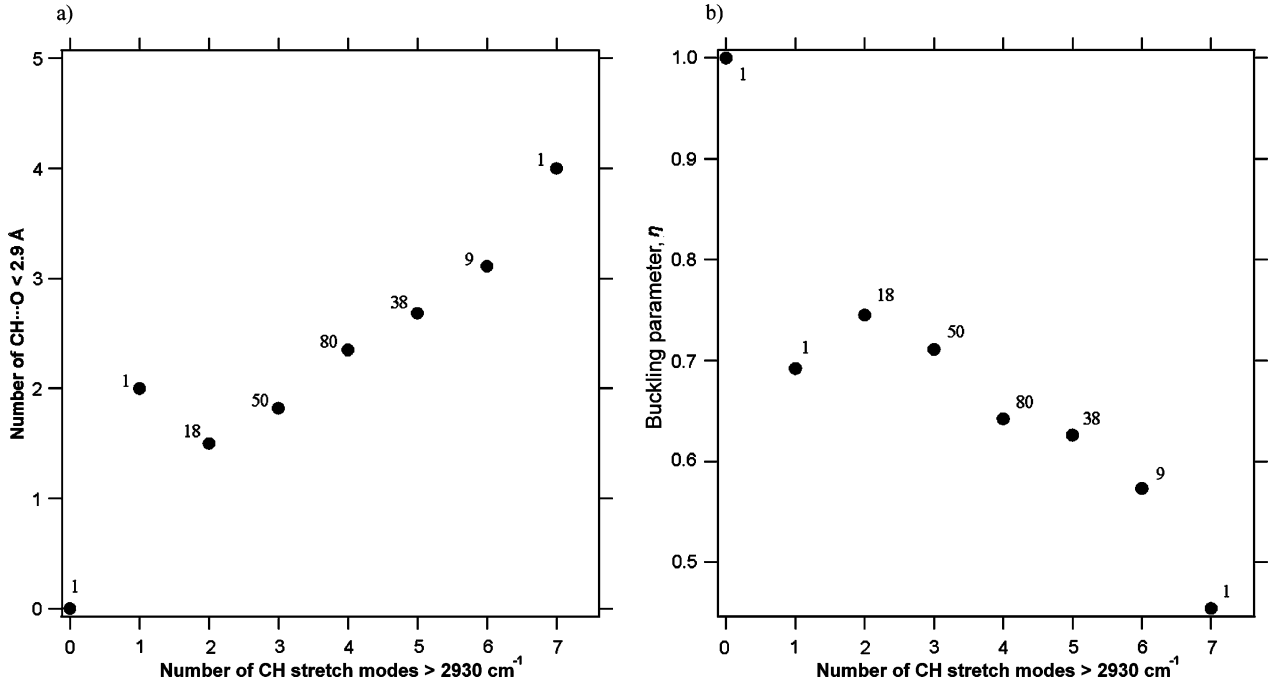

Figure 9. (a) Plot of average number of CH···O interactions (defined as H···O distance <2.9 Å) versus the number of CH modes with fundamental frequency above 2930 cm^{-1}. Numbers next to each point give the number of structures at each *x*-axis point. (b) Plot of average buckling parameter, η, of the crown cycle vs number of CH modes with fundamental frequency above 2930 cm^{-1}. Numbers next to each point give the number of structures at each *x*-axis point.

common conformers that track one another in every detail. On the other hand, calculations based on a harmonic analysis with no account of Fermi resonances are incapable of accounting for the observed spectra quantitatively. In the present work, we have used the high-frequency end of the spectrum as a diagnostic, very generally, of the degree of buckling of the crown. This structural deduction is based on the known effect of CH···O interactions in shifting the CH stretch frequency toward higher wavenumber.

Furthermore, despite a lack of quantitative agreement, the highest frequency CH stretch frequencies from the calculations are almost always associated with CH groups with a potential for involvement in a CH···O interaction, as shown pictorially in Figures 6 and 7. In structures where they are absent, such as the open structure of B15C-X, no high-frequency CH stretch transitions were calculated to be present (see Figure 5, bottom). Indeed, the crown structures associated with B15C-V and B15C-VII both have structures that place a single CH group in close proximity with the lone pairs of both oxygens on the aromatic ring (Figure 6a,b), consistent with the single strong CH stretch transition near 2950 cm^{-1} in the observed RIDIR spectra of B15C(A)/ABC(C) and B15C(B)/ABC(B). A structure like B15C-I has even greater buckling (Figure 6c), placing as many as four CH groups in reasonably close proximity to ether oxygens, qualitatively consistent with the observed triplet of CH stretch transitions near 2950 cm^{-1} in B15C(C) and ABC(A,D).

In point of fact, the present results cannot deduce with certainty whether the characteristic CH stretch transitions observed on the high-frequency edge of the single-conformer spectra are due to CH···O interactions, or are instead the result of the local configurations of the crown that result from the buckling itself. However, an atoms in molecules analysis (AIM), as implemented in GAUSSIAN03,[48] does find interactions with properties consistent with those of hydrogen bonds.[60] One of the unique features of CH···O H-bonds is the contraction of the C−H bond in response to the interaction with the electronegative atom[57] and indeed the CH bonds in the crown cycles identified as taking part in CH···O H-bonds are approximately 0.5% shorter than other CH bonds in the cycle. Another feature of CH···O H-bonds is a decrease in intensity of the blue-shifted transition.[57] In the crown ether alkyl CH spectra, the bands we associate with the CH···O interactions are as intense as any of the other features in the region. However, the CH stretch transitions of the methylene hydrogens involved in these interactions may appear artificially intense if the lower frequency transitions are split by Fermi resonances in a way that the high-frequency transitions are not.

The large number of optimized structures allows us to further investigate the association between the blue-shifted CH stretches and the crown cycle structural geometry. Figure 9a presents a plot of the average number of CH···O interactions versus the number of CH modes above 2930 cm^{-1} and shows a nearly linear correlation between the two parameters. This correlation strongly suggests that the blue-shifted CH stretches we observe are indeed induced by CH···O hydrogen bonds.

In reflecting on our results, we have devised a method of describing how "open" a particular crown conformation is relative to the most "buckled" and most "open" structures found during our conformation searches. The center of the 15-crown-5 ether heavy atom (C or O) architecture was defined as the average position of the atoms in the crown cycle,

$$r_{\text{center}}(i) = \frac{1}{15}\sum_{j=1}^{15} r_j(i)$$

where *j* denotes a heavy atom in the crown cycle and *i* denotes one of the Cartesian axes. The distances of each crown cycle

heavy atom from r_{center}, shown in Figure 7a for B15C-X, were averaged without mass-weighting to give r_{avg}. Smaller r_{avg} values correspond to more "buckled" structures. Drawing from the set of 1698 unique structures, a "buckling" parameter, η, was then calculated using eq 1, where r_{avg} is the average distance as described above, r_{max} is the maximum average distance (corresponding to the most "open" structure), and r_{min} is the minimum average distance (corresponding to the most "buckled" structure). Thus the most "buckled" structure has $\eta = 0$ while the most "open" structure has $\eta = 1$. Smaller η values correspond with more "buckled" structures.

$$\eta = \frac{r_{avg} - r_{min}}{r_{max} - r_{min}} \quad (1)$$

Figure 9b gives the "buckling" parameter, η, as a function of the number of CH modes above 2930 cm^{-1}, again displaying a nearly linear trend and thus indicating that the amount that the crown cycle is "buckled" can be inferred from the number of sharp, blue-shifted CH stretch fundamentals observed in the alkyl CH stretch infrared spectra.

The present results have provided spectroscopic evidence that, in the absence of a binding partner under isolated molecule conditions, the two 15-crown-5 molecules, B15C and ABC, both show substantial buckling of the crown structure to maximize the number and strength of stabilizing CH···O and dispersive interactions between the different segments of the crown macrocycle. As will be presented in the following paper,[33] complexation of a single water molecule to the 15-crown-5 macrocycle opens up the cycle to a conformation not represented among the water-free structures studied here.

Acknowledgment. V.A.S., W.H.J., and T.S.Z. acknowledge the National Science Foundation (CHE-0551075) for financial support of this research. Information Technology at Purdue-the Rosen Center for Advanced Computing (RCAC) and GridChem (http://www.gridchem.org)[67,68] are acknowledged the computational resources employed for this research. V.A.S. acknowledges Bryan Putnam at RCAC for providing invaluable advice that aided the completion of the calculations for this research.

Supporting Information Available: Complete discussion of the TDDFT study performed on singly and doubly substituted alkoxybenzenes, an explanation of the naming scheme used in Table 1, more detail about the TDDFT results on aminophenol derivatives, and the affect that amino substitution has on shifting the electronic origins of alkoxybenzenes are available. This material is available free or charge via the Internet at http://pubs.acs.org/JPCA.

References and Notes

(1) Pedersen, C. J. *J. Am. Chem. Soc.* **1967**, *89*, 7017.
(2) Lehn, J. M. *Pure Appl. Chem.* **1979**, *51*, 979.
(3) Pedersen, C. J. *Science* **1988**, *241*, 536.
(4) Khairutdinov, R. F.; Hurst, J. K. *Langmuir* **2004**, *20*, 1781.
(5) Shinkai, S.; Ogawa, T.; Nakaji, T.; Manabe, O. *J. Chem. Soc., Chem. Commun.* **1980**, 375.
(6) Delmau, L. H.; Bonnesen, P. V.; Engle, N. L.; Haverlock, T. J.; Sloop, F. V.; Moyer, B. A. *Solvent Extr. Ion Exch.* **2006**, *24*, 197.
(7) Ivanyi, T.; Lazar, I. *Synthesis-Stuttgart* **2005**, 3555.
(8) Zhu, L. Y.; Tay, C. B.; Lee, H. K. *J. Chromatogr., A* **2002**, *963*, 231.
(9) Magri, D. C.; Brown, G. J.; McClean, G. D.; de Silva, A. P. *J. Am. Chem. Soc.* **2006**, *128*, 4950.
(10) Kume, S.; Nishihara, H. *Photofunctional Transition Metals Complexes* **2007**, *123*, 79.
(11) Kumondai, K.; Toyoda, M.; Ishihara, M.; Katakuse, I.; Takeuchi, T.; Ikeda, M.; Iwamoto, K. *J. Chem. Phys.* **2005**, *123*, 024314.
(12) Al-Rusaese, S.; Al-Kahtani, A. A.; El-Azhary, A. A. *J. Phys. Chem. A* **2006**, *110*, 8676.
(13) Belkin, M. A.; Yarkov, A. V. *Spectrochim. Acta, Part A* **1996**, *52*, 1475.
(14) Egyed, O.; Izvekov, V. P. *Spectrosc. Lett.* **1989**, *22*, 387.
(15) ElEswed, B. I.; Zughul, M. B.; Derwish, G. A. W. *J. Inclusion Phenom. Mol. Recognit. Chem.* **1997**, *28*, 245.
(16) ElEswed, B. I.; Zughul, M. B.; Derwish, G. A. W. *Spectrosc. Lett.* **1997**, *30*, 527.
(17) Endicott, C.; Strauss, H. L. *J. Phys. Chem. A* **2007**, *111*, 1236.
(18) Kusaka, R.; Inokuchi, Y.; Ebata, T. *Phys. Chem. Chem. Phys.* **2007**, *9*, 4452.
(19) Rogers, R. D.; Kurihara, L. K.; Richards, P. D. *J. Chem. Soc., Chem. Commun.* **1987**, 604.
(20) Rogers, R. D.; Richards, P. D. *J. Inclusion Phenom.* **1987**, *5*, 631.
(21) Wu, Y. J.; An, H. Y.; Tao, J. C.; Bradshaw, J. S.; Izatt, R. M. *J. Inclusion Phenom. Mol. Recognit. Chem.* **1990**, *9*, 267.
(22) Zhelyaskov, V.; Georgiev, G.; Nickolov, Z.; Miteva, M. *Spectrochim. Acta, Part A* **1989**, *45*, 625.
(23) Georgiev, G.; Nikolov, J.; Nickolov, Z.; Zhelyaskov, V. *Spectrochim. Acta, Part A* **1991**, *47*, 749.
(24) Kolthoff, I. M.; Chantooni, M. K. *Can. J. Chem.* **1992**, *70*, 177.
(25) Al-Jallal, N. A.; Al-Kahtani, A. A.; El-Azhary, A. A. *J. Phys. Chem. A* **2005**, *109*, 3694.
(26) Fukushima, K. *Bull. Chem. Soc. Jpn.* **1990**, *63*, 2104.
(27) Jagannadh, B.; Kunwar, A. C.; Thangavelu, R. P.; Osawa, E. *J. Phys. Chem.* **1996**, *100*, 14339.
(28) Paulsen, M. D.; Hay, B. P. *J. Mol. Struct.: THEOCHEM* **1998**, *429*, 49.
(29) Paulsen, M. D.; Rustad, J. R.; Hay, B. P. *J. Mol. Struct.: THEOCHEM* **1997**, *397*, 1.
(30) Jagannadh, B.; Sarma, J. A. R. P. *J. Phys. Chem.* **1999**, *103*, 10993.
(31) Zehnacker, A.; Lahmani, F.; Breheret, E.; Desvergne, J. P.; BouasLaurent, H.; Germain, A.; Brenner, V.; Millie, P. *Chem. Phys.* **1996**, *208*, 243.
(32) Shubert, V. A.; Baquero, E. E.; Clarkson, J. R.; James, W. H.; Turk, J. A.; Hare, A. A.; Worrell, K.; Lipton, M. A.; Schofield, D. P.; Jordan, K. D.; Zwier, T. S. *J. Chem. Phys.* **2007**, *127*, 234315.
(33) Shubert, V. A.; Müller, C.; Zwier, T. S. *J. Phys. Chem. A*, following article in this issue, DOI: 10.1021/jp904233y.
(34) Dian, B. C.; Longarte, A.; Winter, P. R.; Zwier, T. S. *J. Chem. Phys.* **2004**, *120*, 133.
(35) Stearns, J. A.; Das, A.; Zwier, T. S. *Phys. Chem. Chem. Phys.* **2004**, *6*, 2605.
(36) Page, R. H.; Shen, Y. R.; Lee, Y. T. *J. Chem. Phys.* **1988**, *88*, 4621.
(37) Pribble, R. N.; Zwier, T. S. *Science* **1994**, *265*, 75.
(38) Becke, A. D. *J. Chem. Phys.* **1993**, *98*, 5648.
(39) Lee, C. T.; Yang, W. T.; Parr, R. G. *Phys. Rev. B* **1988**, *37*, 785.
(40) Moller, C.; Plesset, M. S. *Phys. Rev.* **1934**, *46*, 618.
(41) Halgren, T. A. *J. Comput. Chem.* **1996**, *17*, 616.
(42) Halgren, T. A. *J. Comput. Chem.* **1996**, *17*, 553.
(43) Halgren, T. A. *J. Comput. Chem.* **1996**, *17*, 520.
(44) Halgren, T. A. *J. Comput. Chem.* **1996**, *17*, 490.
(45) Halgren, T. A.; Nachbar, R. B. *J. Comput. Chem.* **1996**, *17*, 587.
(46) Mohamadi, F.; Richards, N. G. J.; Guida, W. C.; Liskamp, R.; Lipton, M.; Caufield, C.; Chang, G.; Hendrickson, T.; Still, W. C. *J. Comput. Chem.* **1990**, *11*, 440.
(47) Log files available from authors upon request.
(48) Frisch, M. J.; Trucks, G. W.; Schlegel, H. B.; Scuseria, G. E.; Robb, M. A.; Cheeseman, J. R.; Montgomery, J. A., Jr.; Vreven, T.; Kudin, K. N.; Burant, J. C.; Millam, J. M.; Iyengar, S. S.; Tomasi, J.; Barone, V.; Mennucci, B.; Cossi, M.; Scalmani, G.; Rega, N.; Petersson, G. A.; Nakatsuji, H.; Hada, M.; Ehara, M.; Toyota, K.; Fukuda, R.; Hasegawa, J.; Ishida, M.; Nakajima, T.; Honda, Y.; Kitao, O.; Nakai, H.; Klene, M.; Li, X.; Knox, J. E.; Hratchian, H. P.; Cross, J. B.; Bakken, V.; Adamo, C.; Jaramillo, J.; Gomperts, R.; Stratmann, R. E.; Yazyev, O.; Austin, A. J.; Cammi, R.; Pomelli, C.; Ochterski, J. W.; Ayala, P. Y.; Morokuma, K.; Voth, G. A.; Salvador, P.; Dannenberg, J. J.; Zakrzewski, V. G.; Dapprich, S.; Daniels, A. D.; Strain, M. C.; Farkas, O.; Malick, D. K.; Rabuck, A. D.; Raghavachari, K.; Foresman, J. B.; Ortiz, J. V.; Cui, Q.; Baboul, A. G.; Clifford, S.; Cioslowski, J.; Stefanov, B. B.; Liu, G.; Liashenko, A.; Piskorz, P.; Komaromi, I.; Martin, R. L.; Fox, D. J.; Keith, T.; Al-Laham, M. A.; Peng, C. Y.; Nanayakkara, A.; Challacombe, M.; Gill, P. M. W.; Johnson, B.; Chen, W.; Wong, M. W.; Gonzalez, C.; Pople, J. A. *Gaussian 03*, revision C.02, revision C.02; Gaussian, Inc.: Wallingford, CT, 2004.
(49) McQuarrie, D. A.; Simon, J. D. *Molecular Thermodynamics*; University Science Books: Sausalito, CA, 1999.
(50) Hättig, C.; Weigend, F. *J. Chem. Phys.* **2000**, *113*, 5154.
(51) Kusaka, R.; Inokuchi, Y.; Ebata, T. *Phys. Chem. Chem. Phys.* **2008**, *10*, 6238.

(52) Yi, J. T.; Ribblett, J. W.; Pratt, D. W. *J. Phys. Chem. A* **2005**, *109*, 9456.
(53) Please see Supporting Information.
(54) Shinozaki, M.; Sakai, M.; Yamaguchi, S.; Fujioka, T.; Fujii, M. *Phys. Chem. Chem. Phys.* **2003**, *5*, 5044.
(55) Wategaonkar, S.; Doraiswamy, S. *J. Chem. Phys.* **1996**, *105*, 1786.
(56) Robinson, T. W.; Kjaergaard, H. G.; Ishiuchi, S. I.; Shinozaki, M.; Fujii, M. *J. Phys. Chem. A* **2004**, *108*, 4420.
(57) Hermansson, K. *J. Phys. Chem. A* **2002**, *106*, 4695.
(58) Hobza, P.; Havlas, Z. *Chem. Rev.* **2000**, *100*, 4253.
(59) Scheiner, S.; Kar, T. *J. Phys. Chem. A* **2002**, *106*, 1784.
(60) Bader, R. F. W. *Atoms in Molecules. A Quantum Theory*; Clarendon Press: Oxford, U.K., 1990.
(61) Clarkson, J. R.; Baquero, E.; Shubert, V. A.; Myshakin, E. M.; Jordan, K. D.; Zwier, T. S. *Science* **2005**, *307*, 1443.
(62) Clarkson, J. R.; Baquero, E.; Zwier, T. S. *J. Chem. Phys.* **2005**, *122*, 214312.
(63) Clarkson, J. R.; Dian, B. C.; Moriggi, L.; DeFusco, A.; McCarthy, V.; Jordan, K. D.; Zwier, T. S. *J. Chem. Phys.* **2005**, *122*, 214311.
(64) Dian, B. C.; Clarkson, J. R.; Zwier, T. S. *Science* **2004**, *303*, 1169.
(65) Selby, T. M.; Clarkson, J. R.; Mitchell, D.; Fitzpatrick, J. A. J.; Lee, H. D.; Pratt, D. W.; Zwier, T. S. *J. Phys. Chem. A* **2005**, *109*, 4484.
(66) Dian, B. C.; Longarte, A.; Mercier, S.; Evans, D. A.; Wales, D. J.; Zwier, T. S. *J. Chem. Phys.* **2002**, *117*, 10688.
(67) Milfeld, K.; Guiang, C.; Pamidighantam, S.; Giuliani, J. *Cluster Computing through an Application-oriented Computational Chemistry Grid; Proceedings of the 2005 Linux Clusters: The HPC Revolution*, Linux Clusters Institute, 2005.
(68) Dooley, R.; Allen, G.; Pamidighantam., S. *Computational Chemistry Grid: Production Cyberinfrastructure for Computational Chemistry; Proceedings of the 13th Annual Mardi Gras Conference*, Louisiana State University: Baton Rouge, LA, 2005.

JP904231D